

## Two types of ionospheric disturbances in the auroral region<sup>\*</sup>

Shen Changshou (沈长寿)

*Department of Geophysics, Peking University, Beijing 100871, China*

Zi Minyun (资民筠)

*The Academy of Arts of China, Beijing 100009, China*

K. Schlegel

*Max-Planck-Institut für Aeronomie, D-37191, Germany*

Received November 11, 1996

**Abstract** The EISCAT data are used to confirm the important role of precipitation particles in the ionization rate in the auroral region. The height range of the effective ionization is quite different for particles with different energies. On the other hand, an enhancement of magnetospheric convection often results in decreasing of electron density,  $N$ , in the F-layer. During January 28~29, 1985, the disturbed profiles of  $N$  were very typical, in which  $N_m(\text{E-layer}) \gg N(\text{F-layer})$  and  $N$  decreased with height above 147 km. This phenomenon is caused by both energetic particles and intensive convection. During the period of February 16~17, 1993, however, the  $N(\text{F-layer})$  increased extremely, while  $N(\text{E-layer})$  remained low. This is also a typical profile, but is opposite to the former one. In this case, the particles with lower energy ( $< 1$  keV) in the magnetosheath enter directly the high latitude ionosphere through the cusp, and can contribute significantly to the F-layer ionization content.

**Key words** precipitation particles, magnetospheric convection, cusp, auroral ionosphere.

### 1 Introduction

The ionosphere of the auroral region is influenced directly by the solar wind and magnetospheric disturbance. The temporal and spatial variations in the auroral ionosphere are very different from that of the mid- and low-latitude ones. The physical processes which control electron/ion density  $N$  is still the continuity equation:

$$\partial N / \partial t = q - L + \text{div}(N\mathbf{V})$$

Here  $q$  is the production rate of electron/ion,  $L$  is the loss rate and  $\mathbf{V}$  is the plasma velocity. In the mid-latitude ionosphere the production rate  $q$  is almost completely dependent on solar EUV radiation. Therefore, the diurnal, seasonal and latitudinal variations are all very regular. The situation, however, is different when the auroral

---

<sup>\*</sup> This project was supported by National Natural Science Foundation of China.

region is concerned. In this region the precipitation particles from the magnetosphere can be a major source of ionization; during the polar night they are even the only one. On the geomagnetic noonside between  $\Lambda 75^\circ$  and  $\Lambda 80^\circ$ , which area is called the cusp, the solar wind particles (strictly speaking, the magnetosheath plasma) can directly enter the ionosphere.

The normal value of  $V$  at mid-latitudes is about 100 m/s, while in the auroral ionosphere the plasma velocity (which is the sum of three components: diffusion, motion induced by neutral air wind, and  $(\mathbf{E} \times \mathbf{B})/\mathbf{B}$  drift caused by electric field. The latter one is dominating in polar regions) can often be as high as 1~2 km/s. It implies that the transport term  $\text{div}(\mathbf{NV})$  is of particular important. Furthermore, for the mid-latitude F-layer the horizontal derivatives can be negligible and leaves only  $\partial(NV_z)/\partial Z$ ; while in the auroral region  $V$  is so high that the effect of horizontal transport should be included. Finally, the loss rate  $L$  in the F-layer is  $\beta N$ ;  $\beta$  is called the recombination coefficient, which is determined by the collision frequency controlled by the relative speed between the colliding ion and neutral. It does not matter whether the speed is caused by high temperature or by a fast convection. In fact, the effect of an increasing relative velocity of 1 km/s is equivalent to a temperature increase of about 1000 K, which makes ion/neutral reaction faster.

Both the magnetospheric convection and particle precipitation will strengthen during a strong geomagnetic storm. Due to their combining effect the features of the auroral ionosphere become very complex. The particles with energy larger than 10 keV can precipitate to the altitude of 100 km (Banks *et al.* 1974a) and make electron density  $N$  in the E-layer increase dramatically, while the effect of convection enhancement often causes a decreasing of electron density  $N$  in the F-layer. As a result, one will see the phenomenon that  $N_m(\text{E-layer}) \gg N(\text{F-layer})$  in the auroral region when magnetic storms are very strong. This feature is confirmed by incoherent scatter radar observations (Jones 1981; Shen *et al.* 1989). On the other hand, the altitude, where the ionization rate caused by low-energy particles (so called soft particles with energy less than 1 keV) attains its maximum, is in F-layer. These soft particles can precipitate through the cusp into the upper atmosphere on geomagnetic noonside and make  $N(\text{F-layer})$  increase significantly (Whittaker 1976; Titheridge 1976).

In this paper two cases are analyzed to show the disturbed features of the auroral ionosphere caused by various processes.

## 2 The background of geomagnetic activity

Both cases discussed here (Jan. 27~29, 1985 and Feb. 16~18, 1993) are in winter of low solar activity years. The extremely negative values of  $D_{st}$  are  $-117$  and  $-108$  nT, respectively. The  $D_{st}$  indices during these two main phases are very variable. The variations of the geomagnetic indices concerned during the storms are shown in Fig. 1.

During the storm in Jan. 1985, when the main phase started at 0:00 UT on 28th, the value of  $D_{st}$  stayed between  $-20$  nT and  $-30$  nT and it did not decrease

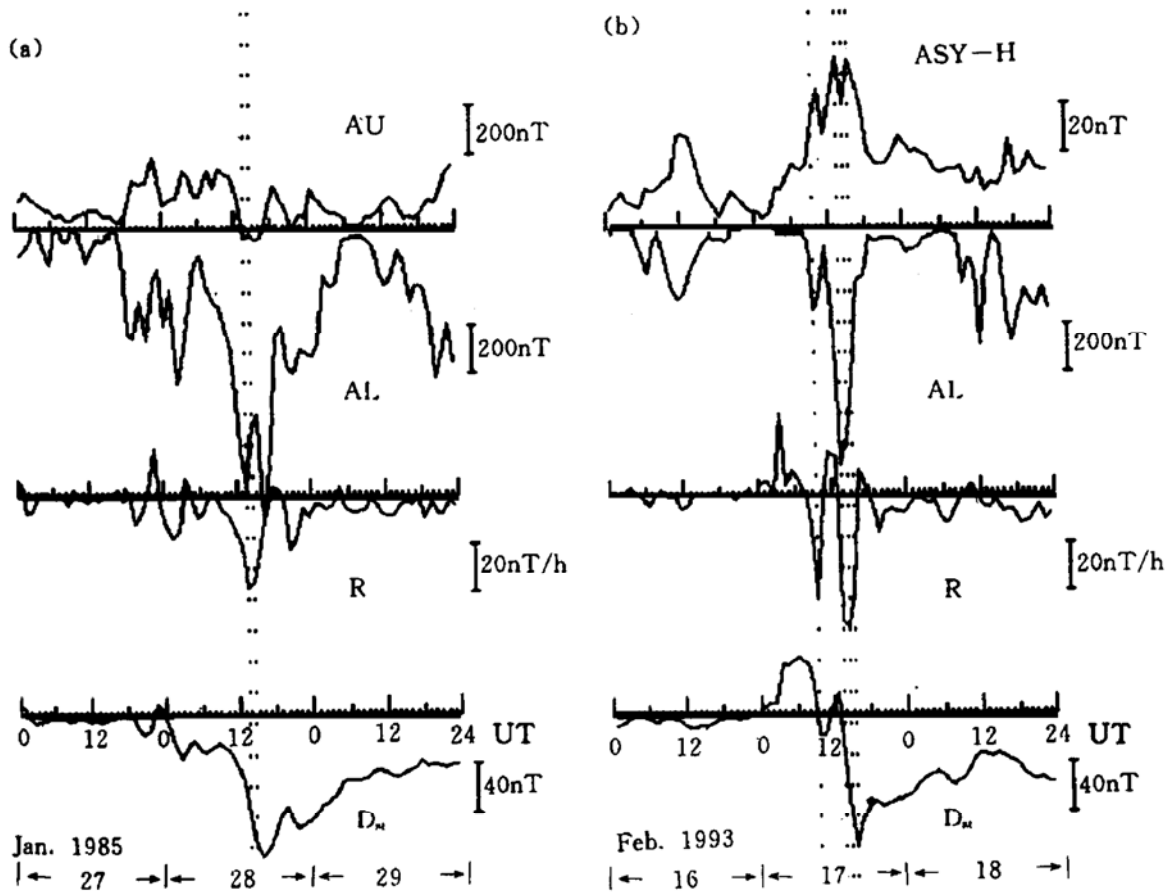


Fig. 1. Variations of  $D_{st}$ ,  $R$ ,  $AL$  and  $AU$  during 27~29 Jan. 1985(a) and  $D_{st}$ ,  $R$ ,  $AL$  and  $ASY-H$  during 16~18 Feb. 1993(b).

dramatically until 12:00 UT. Corresponding to this, the inflation rate of the ring current (the  $R$  index) was only  $-18$  nT/h at 1:00 UT. This value is higher than the low limit of the so-called  $R$  event ( $R < -25$  nT/h); at 13:00 UT  $R = -38$  nT/h, that implies a great amount of energy releases from the inner magnetosphere into the auroral ionosphere by means of the region 2 field-aligned current. At the same time, the extreme value of the auroral electrojet index  $AL$  (westward) attained to  $-1229$  nT, while the  $AU$  index (eastward electrojet) decreased to  $-49$  nT, which usually has a positive value.

These phenomena indicate that both magnetospheric convection and particle precipitation are so strong, that on the night side not only the westward auroral electrojet increases significantly, but the eastward one also decreases greatly owing to the westward rotation of the two-cell convection pattern, and the value of  $AU$  turns to negative sometimes.

The storm in Feb. 1993 started at 0:00 UT on 17-th with positive  $D_{st}$ . During the first initial phase  $D_{st}$  remained larger than 40 nT for 5 h (4:00~8:00 UT). Then, not too long time later, at 12:00~13:00 UT  $D_{st}$  turned to positive again (that means a second initial phase started). Corresponding to the two main phases,  $R$  index turned to negative dramatically twice:  $R(9:00 \text{ UT}) = -41.4$  nT/h and  $R(14:00 \text{ UT}) = -54.2$  nT/h (in Fig. 1a and 1b, the time when  $R < -25$  nT/h is marked by a long vertical dotted line). The effects of these two energy releases from the ring cur-

rent can be seen from the variations of  $AL$  and  $ASY-H$ , which is used for describing the longitudinally asymmetric disturbance of  $H$ -component in mid-latitudes (Iyemori 1992). The extreme values are  $-330$  nT and  $57$  nT, respectively, for the first main phase; and  $-975$  nT and  $71$  nT for the second one.

### 3 The features of the ionosphere in the auroral region

As mentioned above, the solar activity and geomagnetic variation of the two cases are very similar. However, the corresponding disturbances in the auroral ionosphere observed by the EISCAT radar at Tromso, Norway, show various features.

#### 3.1 Vertical profile of electron density

The data used here are observed by EISCAT using common program 1 (CP-1). For the case of 1985 during the period between 12:40 UT on Jan. 28 and 11:50 UT on Jan. 29, the time resolution of observation is 5 min. The parameters recorded are uncorrect electron density  $N_0$  between  $79 \sim 200$  km spaced at  $1.5$  km and the true density  $N$ , electron and ion temperature:  $T_e, T_i$  and the line-of-sight velocity along the radar beam  $V_L$  between  $147 \sim 585$  km spaced at  $22$  km. The profiles of  $N$  with interval of 15 min during period of 12:40~24:00 UT on Jan. 28 are shown in Fig. 2a. The lower parts of each curve represent the uncorrect  $N_0$  between  $97 \sim 150$  km, while the upper ones give the true density  $N$  above  $147$  km. Since the signal-to-noise ratio

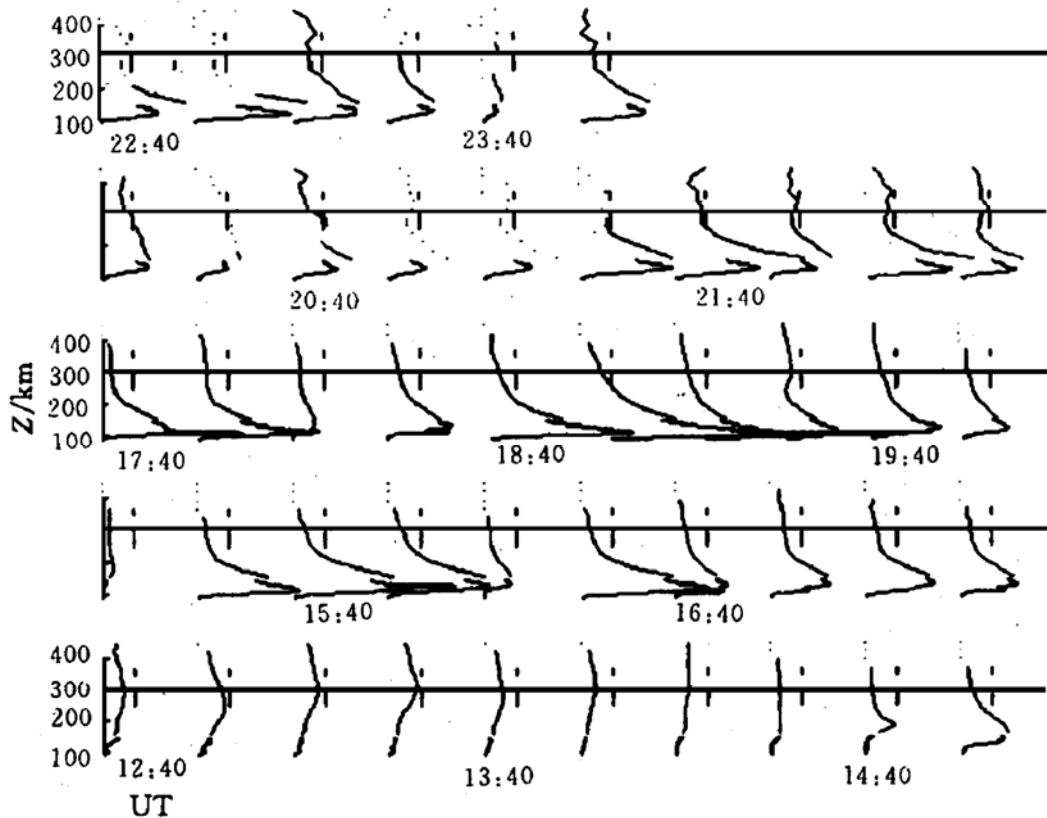


Fig. 2a. The profiles of  $N$  between  $90$  km and  $400$  km during 12:40~24:00 UT on 28 Jan. 1985.

is too small for most records above 400 km, they are not shown in Fig. 2a. The dotted curves also indicate this kind of unbelievable records between 147~400 km. The location of  $N = 1 \times 10^{11}$  el./m<sup>3</sup> is given by a vertical short line for each curve. According to the principle of EISCAT observation,  $N_0$  is very close to the true  $N$  if  $T_e \simeq T_i$ . For such circumstance, the profile of  $N$  above 150 km links well with that below 150 km. So, one could see a continuous distribution curve. On the other hand, when the energetic particles increase dramatically,  $T_e$  will be much higher than  $T_i$ . In this case  $N_0 \ll N$ , that means  $N_0$  below 150 km is much less than the true value. It is why the curves after 15:00 UT are not continuous. Nevertheless, the variation trend of  $N_0$  can still reflect the fundamental physical feature of processes.

It can be seen from Fig. 2a that the values of  $N_0$  around 110 km are often larger than  $2 \times 10^{11}$  el./m<sup>3</sup> after 15:25 UT and reach to  $6 \times 10^{11}$  el./m<sup>3</sup> at 19:00 UT. On the other hand,  $N$  is less than  $1 \times 10^{11}$  el./m<sup>3</sup> above 200 km, and its value decreases when the altitude increases. The Chapman distribution form of density in the F-layer disappears entirely. The physical background of this phenomenon has been mentioned in the introduction, i. e. the combining effect of the increasing ionization in the E-layer caused by the particle precipitation and the speeding up of ion recombination in F-layer due to the enhancement of convection. In fact,  $N_m(\text{E-layer}) \gg N(\text{F-layer})$  is a typical profile in the auroral region during storms. This feature can also be seen from the  $N$  profile of the case on Jan. 29, which has not been shown here since the paper

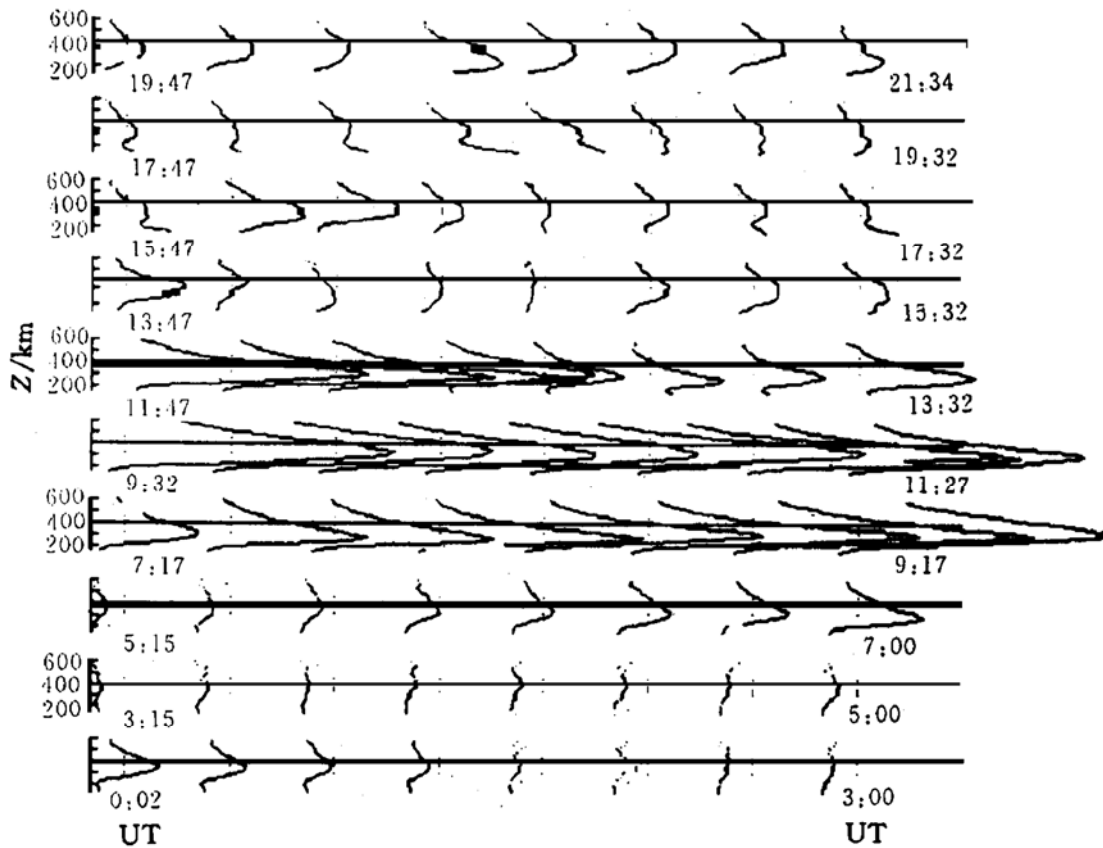


Fig. 2b. The profiles of  $N$  between 147 km and 585 km during 0:00~22:00 UT on 17 Feb. 1993.

length is limited.

For the case on Feb. 16~17, 1993 we only have data of  $N$ ,  $T_e$ ,  $T_i$  and  $V_L$  between 147~585 km spaced at 22 km. The profiles of  $N$  in period of 0:00~22:00 UT on Feb. 17-th are shown in Fig. 2b for each 15 min. The meanings of the dotted curve and short vertical line are the same as in Fig. 2a. It can be seen that  $N$ (F-layer) increase dramatically in period of 8:30~13:30 UT. The maximum value of  $N$ (F-layer) is  $1 \times 10^{12}$  el./m<sup>3</sup> and its corresponding  $h_m F$  is larger than 300 km. Although there has no data below 147 km, it is still obvious that not any increasing trend of  $N$ (E-layer) can be found from most of the profiles above 147 km. Only after 14:00 UT (15:30 LT), one can see that  $N(147 \text{ km}) > N(350 \text{ km})$  and the F-layer disappears. The observation on Feb. 16 started at 10:00 UT. Again, it is shown that  $N$ (F-layer)  $\sim 1 \times 10^{12}$  el./m<sup>3</sup> and  $N(147 \text{ km}) < 1 \times 10^{11}$  el./m<sup>3</sup> before 14:00 UT (not given here). This phenomenon, obviously, has no relation with the particle precipitation. The enhancement of convection has nothing to do with it, too, since it can only make  $N$ (F-layer) decrease. Now, it is known that the position of the cusp is around  $\Lambda 75^\circ \sim \Lambda 80^\circ$  on the noonside and it can extend to lower latitude during a strong storm. It is believed that the magnetosheath plasma could enter directly the ionosphere. The ionization rate of these soft particles attains its maximum value of  $1 \times 10^{-5} \text{ cm}^{-3} \cdot \text{sec}^{-1}$  at height of 200~400 km (Banks *et al.* 1974a). The latitude of Tromsø Station is  $69.6^\circ$  N. It is lower than that of the normal cusp area, so the ionospheric disturbance in the F-layer caused by soft particles can only be observed at geomagnetic noon during strong storms. Therefore, it is a type of disturbance that is rarely observed.

In fact, 1993 is a year of low solar activity. No solar flare has been recorded in period of Feb. 16~17. This means that the dramatically increasing of  $N_m F$  is not induced by energetic particles, but by soft ones from the magnetosheath.

### 3.2 The maximum electron density of the F-layer and its altitude

To inspect features of the F-layer for these two cases in detail, the variations of the main parameters are investigated.

Fig. 3a shows the evolution of  $N_m F$ ,  $h_m F$  and  $TEC$  (147~400 km) (the total electron content between 147 km and 400 km) in period from 12:40 UT on 28-th to 12:00 UT on 29-th in Jan. 1985. The ionization rate in the E-layer, caused by energetic particles with energy of 10 keV and higher, is about  $1 \times 10^{-4} \text{ cm}^{-3} \cdot \text{sec}^{-1}$ , while the enhancement of convection makes  $N$ (F-layer) decrease and it decreases with increasing of altitude in most night profiles of  $N$  above 147 km, where  $N$  attains its maximum value. One can find that the  $h_m F$  is at 300 km only at daytime when it is still controlled by solar radiation. The ionization at 147 km at night was mainly caused by energetic particle precipitation with a higher rate than that induced by solar EUV radiation at daytime in F-layer. Therefore, in Fig. 3a  $N(147 \text{ km})$  at night are often larger than  $N(300 \text{ km})$  at daytime. The  $TEC(147 \sim 400 \text{ km})$  in Fig. 3a is one order of magnitude less than  $TEC(147 \sim 585 \text{ km})$  in Fig. 3b. Besides the different energy intensity of precipitation particles mentioned above, the fact that the signal-

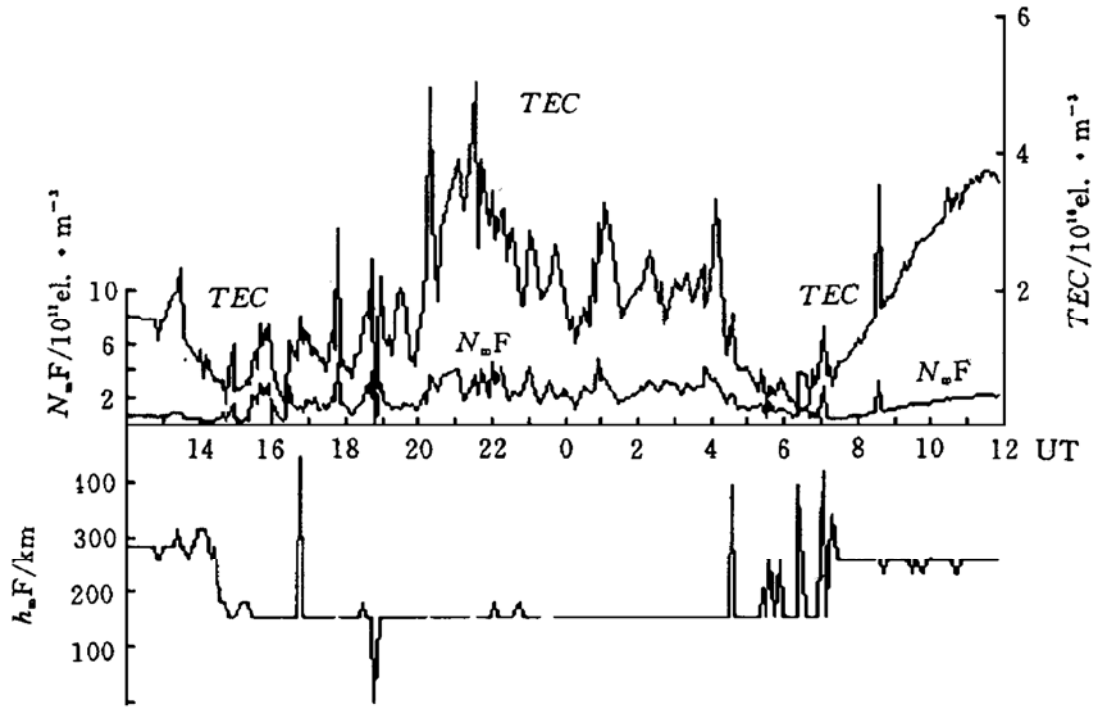


Fig. 3a. Variations of  $N_mF$ ,  $h_mF$  and  $TEC(147\sim400\text{ km})$  during 28~29 Jan. 1985.

to-noise ratios above 400 km in the case of Fig. 3a are often so low that the records are unreliable and excluded, is also a reason that reduces the value of  $TEC$ . Furthermore, there are a couple of isolated abrupt variation which are unreliable too.

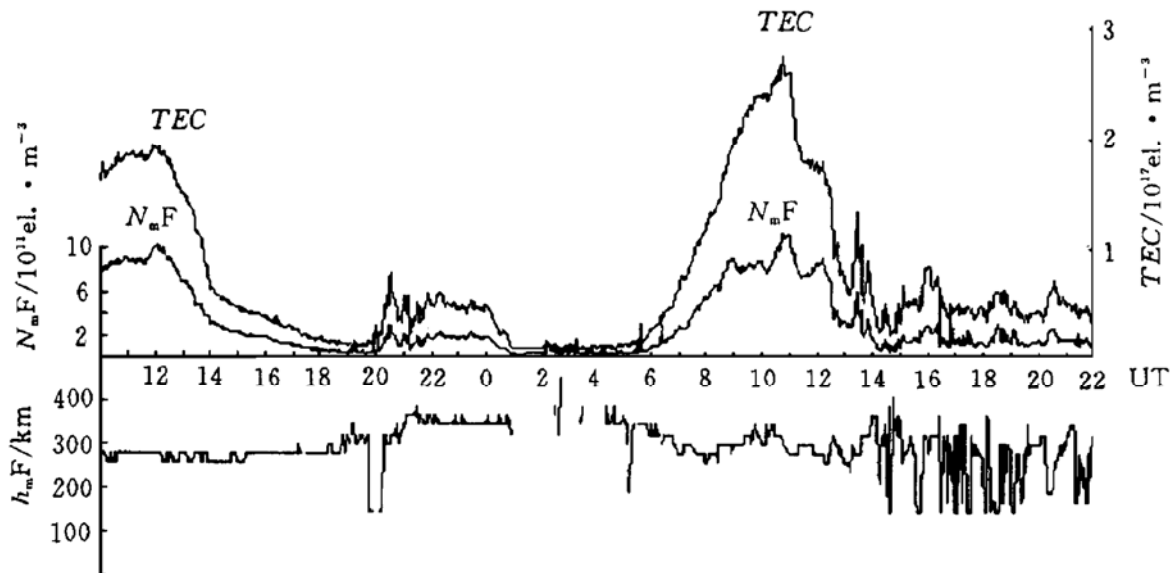


Fig. 3b. Variations of  $N_mF$ ,  $h_mF$  and  $TEC(147\sim585\text{ km})$  during 16~17 Feb. 1993

Fig. 3b gives the corresponding parameter variations for period between 10:00 UT on 16-th and 22:00 UT on 17-th in Feb. 1993. When the observatory entered the

cusps around geomagnetic noon, the ionization caused by soft particles from magnetosheath led to  $N_mF$  and  $TEC$  increase dramatically. Their maximum values are:  $N_mF > 1 \times 10^{12}$  el./m<sup>3</sup> and  $TEC > 3 \times 10^{17}$  el./m<sup>2</sup>. These variations are exactly the same as that in Fig. 2b. (It should be indicated that the increasing of  $N_mF$  and  $TEC$  on the noonside in Fig. 3a is a normal diurnal variation which has nothing to do with precipitation of soft particles. The values of  $N_mF$  and  $TEC$  around noontime in Fig. 3b are one order of magnitude larger than that in Fig. 3a.). In Fig. 3b  $h_mF$  is a bit lower than 300 km at daytime and about 350 km at night, which belongs to normal peak of the F-layer. Both  $N_mF$  and  $TEC$  increase after 14:00 UT on Feb. 17, but  $h_mF$  fluctuates between 147 km and 300 km. This reflects the enhancement of energetic particle ionization and its transient feature. Combining with the simultaneous variation of the relative temporal profiles, one may inspect the whole process of this period in detail.

### 3.3 Ion and electron temperatures and the component of convection velocity

Through the Doppler effect, one can only get one component of velocity along the radar beam (it is roughly parallel to the geomagnetic field line). It has been proved, however, that the variation of  $V_L$  is corresponding to that of the total convection velocity. Therefore, one can deduce the evolution of convection using  $V_L$ .

Fig. 4a shows the variations of  $N$ ,  $V_L$ ,  $T_e$  and  $T_i$  at 338 km for the case in Jan. 1985. In the whole period one can see that  $N < 1 \times 10^{11}$  el./m<sup>3</sup>. Then, the curve of  $N$  is very close to  $X$  coordinate axis. This small value is a result of convection enhancement; here, the fact that the variation range of  $V_L$  is as high as 100 km/s confirms once again that the physical mechanism mentioned above is reasonable.

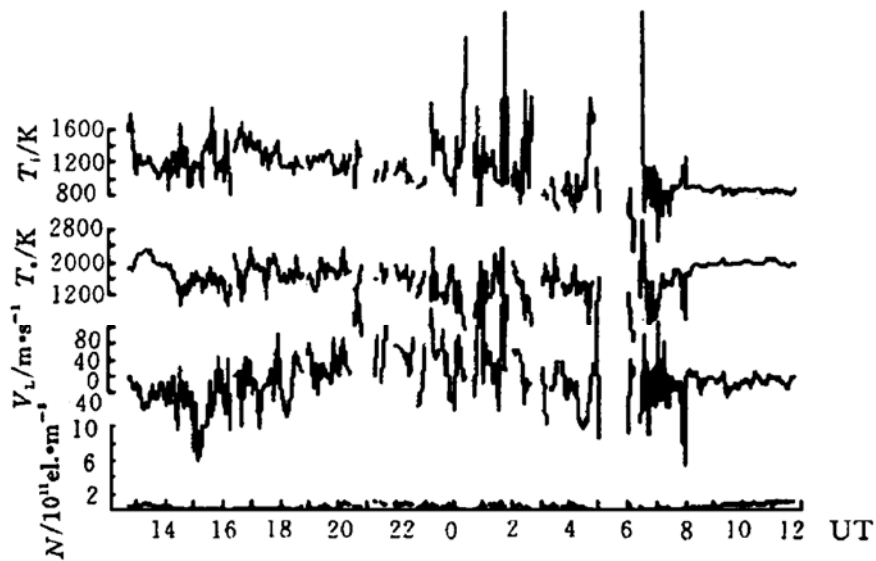


Fig. 4a. Variations of  $N$ ,  $V_L$ ,  $T_e$  and  $T_i$  at 338 km during 28~29 Jan. 1985.

In fact, in the F-layer the most important photochemical processes for the loss of  $O^+$  are:  $O^+ + O_2 \rightarrow O_2^+ + O$  and  $O^+ + N_2 \rightarrow NO^+ + N$ ; then, both  $O_2^+$  and  $NO^+$  turn



to molecule according to  $M^+ + e \rightarrow M$ . The laboratory measurements (McFarland *et al.* 1973) have proved that the reaction rate,  $k$  of  $O^+ + N \rightarrow NO^+ + N$  can be expressed by:

$$\begin{aligned} k &= 1.2 \times 10^{-18} (300/T_{\text{eff}}) \quad (\text{m}^3/\text{s}) & T_{\text{eff}} < 750 \text{ K} \\ k &= 8 \times 10^{-20} (T_{\text{eff}}/300)^2 \quad (\text{m}^3/\text{s}) & T_{\text{eff}} > 750 \text{ K} \end{aligned}$$

Here,  $T_{\text{eff}}$  is called effective temperature. According to Banks *et al.* (1974b):

$$T_{\text{eff}} = T_n + 0.329 E_{\perp}^2$$

$T_n$  is temperature of the neutral atmosphere;  $E_{\perp}$  is the component of the electric field perpendicular to magnetic field, which reflects the increasing relative ion/electron velocity due to  $(\mathbf{E} \times \mathbf{B})/B$  drifts. In fact, an electric field with moderate intensity ( $E = 50 \text{ mV/m}$ ) will make  $k$  increase by a factor of 3.3 (Kohl, 1981). This may let  $N(\text{F-layer})$  reduce significantly.

The positive correlation between  $V_L$  and  $T_i$  can also be seen from Fig. 4a. Viewing from physical theory, the increasing of  $T_i$  is a result of the Joule heating induced by convection enhancement (Banks 1977). The variation of  $T_e$  is more complex. It is mainly controlled by the collision of energetic particles. There are blanks and few abnormal values in Fig. 4a, which are caused by the low signal-to-noise ratio.

Fig. 4b gives the similar picture at 322 km for the case of Feb. 16~17, 1993. As comparing to Fig. 4a, the increasing of  $N(\text{F-layer})$  at noontime is very significant and the values are far beyond the normal  $N(\text{F-layer})$  in winter. On the other hand, the value of  $V_L$  is very small (it means that convection is relatively weak) except the period of dawn and after 13:00 UT. Furthermore,  $T_i$  increases considerably when the variation range of  $V_L$  increases. The variations of these four parameters after 13:00 UT are just a result of the tremendous increasing of both magnetospheric convection and energetic particles.

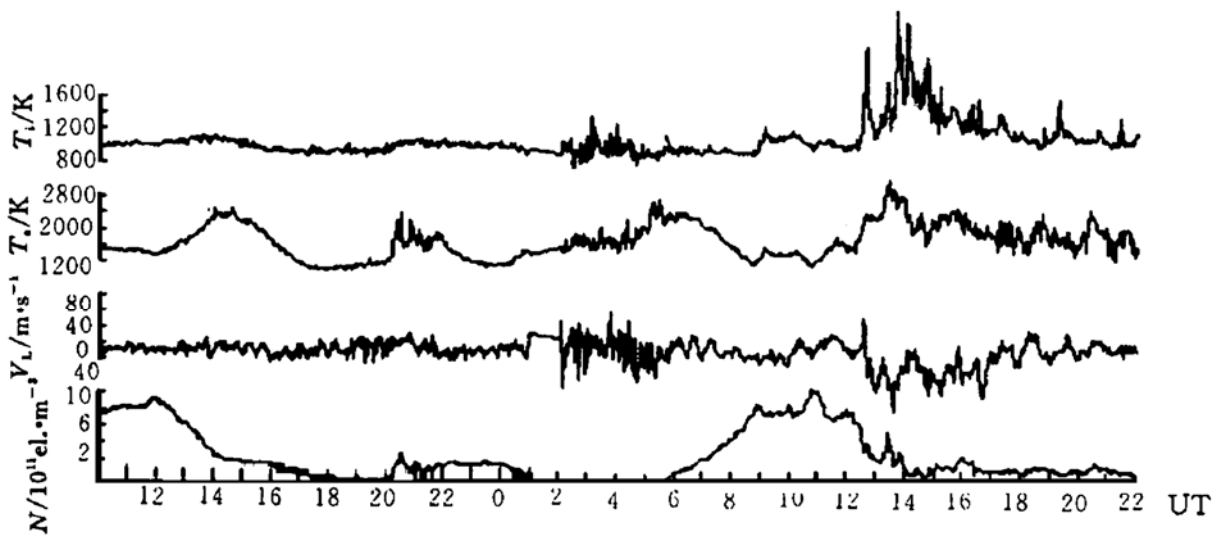


Fig. 4b. Variations of  $N, V_L, T_e$  and  $T_i$  at 322 km during 16~17 Feb. 1993.

#### 4 Brief summary

The analysis of two cases mentioned above indicates that the types of ionospher-

ic disturbance in the auroral region are many and varied.

During the storm on Jan. 28~29, 1985, both convection and energetic particle precipitation are increasing significantly. Their combining effect results in that  $N_m$  (E-layer)  $\gg N$ (F-layer) and  $N$ (F-layer) decreases with altitude's increasing. Therefore, the Chapman distribution of  $N$  in the F-layer does not exist at all. These phenomena are observed by Chatanika and EISCAT radars many times.

During the storm on Feb. 16~17, 1993, however, except afternoon on Feb. 17, no significant convection enhancement can be seen, and  $N$ (E-layer) is much less than  $N_m$ F. On the other hand,  $N$ (F-layer) increase abnormally around noon of these two days. This result can only be interpreted by the effect of soft particles entering the ionosphere from the magnetosheath. Since the station locate beyond the low latitude boundary of the cusp, this kind of disturbance can only be observed occasionally.

In one word, during the two storms although the geomagnetic variation and solar activity are similar, the energy spectrum of precipitation particles and convection are very different. Therefore, not only the disturbed features in high latitude are entirely different from that in the mid-latitude ionosphere where the ionization is mainly controlled by solar EUV radiation, but even in the auroral ionosphere the types of disturbance analyzed above are distinct from each other. This indicates once more that in studying of the magnetosphere-ionosphere coupling, one should collect data from various observations as much as possible to avoid subjectivity and one-sidedness.

## References

- Banks P M, Chappell C R, Nagy A F (1974a): A new model for the reaction of auroral electrons with the atmosphere: spectral degradation backscatter, optical emission and ionization. *J. Geophys. Res.*, 79: 1459~1470.
- Banks P M, Schunk R W, Raitt W J (1974b):  $\text{NO}^+$  and  $\text{O}^+$  in the high latitude F-region. *Geophys. Res. Lett.*, 1: 239~242.
- Banks P M (1977): Observation of Joule and particle heating in the auroral zone. *J. Atmos. Terr. Phys.*, 39: 179~193.
- Iyemori T (1992): Mid-latitude geomagnetic indices "ASY" and "SYM" for 1989~1991. Kyoto University, Japan.
- Jones T B (1981): Radio observations of the auroral F-region. In: *Exploration of the Polar Upper Atmosphere*, Ed. by Deehr C S and Holtel J A, D Reidel Publishing Company, 67~82.
- Kohl H (1981): Polar F-region—Theory. In: *Exploration of the Polar Upper Atmosphere*, Ed. by Deehr C S and Holtel J A, D. Reidel Publishing Company, 55~66.
- McFarland M, Albritton D L, Fehsenfeld F C, Ferguson E E, Schmeltekopf A L (1973): Flowdrift technique for ion mobility and ion-molecule reaction rate constant measurement II: positive ion reactions of  $\text{N}^+$ ,  $\text{O}^+$  and  $\text{N}_2^+$  with  $\text{O}_2$  and  $\text{O}^+$  with  $\text{N}_2$  from thermal to  $\sim 2$  eV. *J. Chem. Phys.*, 59: 6620~6628.
- Shen Changshou, Zi Minyun, K Schlegel (1989): A case study of the ionospheric morphology at high latitude. *Acta Geophysica Sinica*, 32(3): 262~269 (in chinese).
- Titheridge J E (1976): Ionospheric heating beneath the magnetospheric cleft. *J. Geophys. Res.*, 81: 3221~3226.
- Whittaker J H (1976): The magnetospheric cleft-ionospheric effects. *J. Geophys. Res.*, 81: 1279~1288.